THE JOURNAL OF PHYSICAL CHEMISTRY B

Article

pubs.acs.org/JPCB

Tryptophan Rotamer Distribution Revealed for the α-Helix in Tear Lipocalin by Site-Directed Tryptophan Fluorescence

Oktay K. Gasymov,* Adil R. Abduragimov, and Ben J. Glasgow*

Departments of Pathology and Ophthalmology and Jules Stein Eye Institute, University California at Los Angeles, Los Angeles, California 90095, United States

ABSTRACT: Rotamer libraries are a valuable tool for protein structure determination, modeling, and design. Site-directed tryptophan fluorescence (SDTF) was used in combination with the rotamer model for the fluorescence intensity decays to solve α-helical conformations of proteins in solution. Single Trp mutations located in an α-helical segment of human tear lipocalin were explored for structure assignment. Along with fluorescence λ_{max} values, the rotamer model assignment of fluorescence lifetimes fits the backbone conformation. Typically, Trp fluorescence in proteins shows three lifetimes. However, for the α-helix, two lifetimes assigned to t and g^- rotamers were satisfactory to describe Trp fluorescence intensity decays. The g^+ rotamer is not feasible in the α-helix due to steric restriction. Trp rotamer distributions obtained by fluorescence were compared with the rotamer library derived from X-ray crystallography data of proteins. The Trp rotamer distributions vary for solvent exposed and buried (tertiary interaction) sites. A new strategy using the rotamer distribution with SDTF (RD-SDTF) removes the limitation of regular SDTF and other labeling techniques, in which site-specific differences, e.g., accessibility, are presumed. The RD-SDTF technique does not rely on environmental differences of side chains and is able to detect α-helical structure where all side chains are exposed to solvent. Potentially, this technique is applicable to various proteins including membrane proteins, which are rich in α-helix motif.

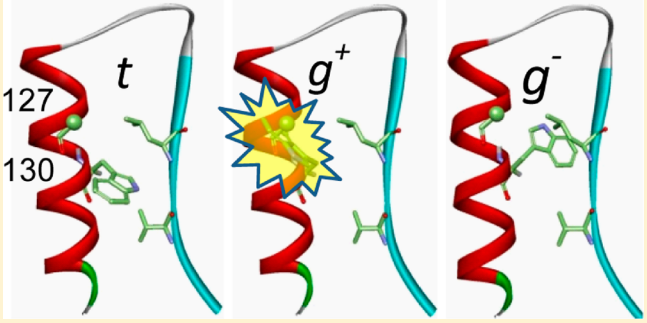

INTRODUCTION

Rotamers reflect discrete side-chain conformations that impact functions of proteins by activation of conformational transitions. An example is the concerted side-chain conformational switch observed for siderophore binding to human NGAL.[1−3] The side-chain rotamer distributions are also invaluable tools for theoretical models of proteins. Access to accurate rotamer information greatly improves both the speed and accuracy of building X-ray crystallographic and theoretical conformation models of protein structure. Systematic advances in understanding Trp fluorescence have boosted fluorescence spectroscopy to be one of the best tools to study Trp rotamers. Site-directed tryptophan fluorescence (SDTF) is a powerful technique to study the relationship of protein structure, dynamics, and function. Trp as a spectroscopic probe has several advantages over others. First, Trp is a natural amino acid and can be introduced to any point of the protein as a probe without the need for chemical labeling. Labels may be hampered by inaccessibility or other environmental features. Second, Trp fluorescence parameters, such as the fluorescence λ_{max} value, quantum yield, and lifetimes, have remarkable sensitivity to Trp's immediate environment.[4] In proteins, fluorescence λ_{max} values of Trp vary within the range of 308−355 nm. This range reflects environments from the most buried and hydrophobic (blue edge) to the fully solvent exposed and polar sites (red edge).[5−7] The local electric field (direction and magnitude) satisfactorily predicts fluorescence λ_{max} value variation in proteins.[7] For the protein tear lipocalin, SDTF has revealed that Trp fluorescence λ_{max} values distributed within range of 313−355 nm.[5]

Significant advances have been made to many aspects of Trp fluorescence.[6,8−14] Extensive studies of Trp fluorescence on conformationally restricted peptides in combination with NMR spectroscopy have enabled the unambiguous assignment of fluorescence lifetimes for a particular rotamer conformation.[11,15,16] The electron transfer (ET) from the excited indole ring to the peptide backbone (nearest C atom of the carbonyl group) is the primary process that discriminates fluorescence lifetimes of each rotamer conformation of Trp.[8,12,13,17] Trp fluorescence can be quenched by side chains of eight amino acids.[8] Both excited-state proton (Lys and Tyr) and electron transfer (Gln, Asn, Glu, Asp, Cys, and His) mechanisms may cause quenching.[8]

Most proteins containing single Trp residues display fluorescence with three lifetimes. A rotamer model in which Trp fluorescence lifetimes are derived from discrete rotamer conformations is widely accepted and has a strong theoretical background. However, the experimental application of this model in proteins is touted to have limitations. Theoretically, possible fast interconversion between rotamer conformations

Received: September 19, 2012
Revised: October 21, 2012
Published: October 22, 2012

and/or multiple backbone conformations (predominantly in the loop regions of the proteins) would blur the lifetime assignment of Trp fluorescence.[10] Yet, the Trp rotamer model was successfully demonstrated in a short peptide, and the structure was modulated by interaction with a phospholipid surface. In the α-helical form, the lifetime distributions of Trp residues positioned sequentially in the peptide corroborate the rotamer distribution library derived from X-ray crystallography data.[18] However, the rotamer model of Trp fluorescence lifetime distribution has not been systematically tested in proteins. TL is an ideal protein to test the rotamer model for lifetime distribution of Trp fluorescence. The solution structure as well as ligand binding mechanism was successfully resolved by SDTF[3,5,19] and verified by crystallography.[20,21] Prior detailed work with SDTF in TL sets the stage for extending its application to rotamer analysis.

Rotamer distributions are important to understand detailed mechanistic and functional information about ligand binding in tear lipocalin. Tear lipocalin (also known as von Ebner's gland protein and LCN1) is the major lipid binding protein in human tears.[22,23] Tear lipocalin binds a wide assortment endogenous (fatty acids, alkyl alcohols, glycolipids, phospholipids, and cholesterol[23,24]) as well as a variety of exogenous ligands.[25−27] A rotamer switch impacts fatty acid binding in tear lipocalin, through protonation/deprotonation of Glu27.[3,19,20] Additionally, Trp17 in tear lipocalin is critical for structural stability and ligand binding.[25,28] The crystal structures of TL support the rotamer assignment of Trp17. Trp17 resides in a very restricted environment. Accordingly, 97% of the fluorescence intensity decay of Trp17 could be assigned to one lifetime, and therefore, one rotamer.[29] Other major rotamers are incompatible with the crystal structures.[20,21] If successfully applied to proteins, tryptophan rotamers may be useful in reporting intricate dynamic changes in the various other functions attributed to TL.

In this work, RD-SDTF was applied to the α-helical region of TL to test the rotamer model of Trp fluorescence in proteins. The rotamer model elucidated with RD-SDTF is potentially applicable to proteins rich with α-helical structure, such as membrane proteins.

EXPERIMENTAL SECTION

Materials. In spectroscopic studies, all materials used in preparation of the dilute solutions of the mutant proteins were purchased from Sigma-Aldrich (St. Louis, MO).

Site-Directed Mutagenesis and Plasmid Construction. Previously synthesized TL cDNA[30] in PCR II (Invitrogen) was the template to clone the TL gene spanning bases 115−592 of the sequence[31] into pET 20b (Novagen, Madison, WI). To produce the native protein sequence as found in tears, flanking restriction sites were added to NdeI and *Bam*HI. However, the initiating methionine was left in place.[32] The previously well-characterized TL mutant, W17Y,[25] was used as a template to construct the mutants with a single Trp. W17Y was prepared with oligonucleotides (Universal DNA Inc., Tigard, OR) by sequential PCR steps.[25,33] Mutant cDNAs in which selected amino acids were additionally substituted with tryptophan were constructed. Amino acid 1 corresponds to His, bases 115−118, according to previously published work.[31]

To test the rotamer model with Trp fluorescence lifetimes in proteins, single Trp mutants of TL that cover the main α-helix were produced. Single Trp mutants of TL include W17Y/L124W (for simplicity denoted as W124); W17Y/E125W (W125); W17Y/A126W (W126); W17Y/L127W (W127); W17Y/E128W (W128); W17Y/D129W (W129); W17Y/F130W (W130); W17Y/E131W (W131); W17Y/K132W (W132); W17Y/A133W (W133); W17Y/A134W (W134); W17Y/G135W (W135); W17Y/A136W (W136); and W17Y/R137W (W137). All mutant proteins have the native fold as previously shown by far-UV circular dichroism.[5]

Expression and Purification of Mutant Proteins. The mutant plasmids were transformed in *E. coli*, BL 21 (DE3), and cells were cultured and proteins were expressed, purified, and analyzed as described in the Supporting Information of refs 5 and 34. The expressed mutant proteins were used without additional enrichment with ligand. Previously, it has been shown that mutant proteins expressed in *E. coli* contain various fatty acids including palmitic acid.[25]

Absorption Spectroscopy. UV absorption spectra of the single Trp mutants of TL were recorded at room temperature using a Shimadzu UV-2400PC spectrophotometer. All experiments were performed in 10 mM sodium phosphate, pH 7.3. To increase accuracy of the quantum yield values of the fluorescence of Trp mutants, the spectra were corrected for light scattering as described elsewhere.[34]

CD Spectral Measurements. Far-UV CD spectra were recorded for all mutants at room temperature on a Jasco J-810 spectropolarimeter. The path length was 0.2 mm. The concentrations of the proteins were about 0.9 mg/mL. Nine scans of each CD spectrum were averaged to improve signal/noise ratio.

Steady-State Fluorescence Spectroscopy. Steady-state fluorescence measurements were made with a JobinYvon-SPEX (Edison, NJ) Fluorolog tau-3 spectrofluorometer. The bandwidths for excitation and emission were 2 and 3 nm, respectively. The excitation λ of 295 nm was used to ensure that light was absorbed almost entirely by a tryptophanyl group. Protein solutions with about 0.07 OD at 295 nm were analyzed. All spectra were obtained from samples in 10 mM sodium phosphate at pH 7.3. The fluorescence spectra were corrected for light scattering from buffer and then for the instrument response by means of the appropriate correction curve. The quantum yields of the Trp residues in the proteins were calculated using a fluorescence standard, NATA (*N*-acetyl-L-tryptophanamide). Quantum yield of NATA was taken as 0.13.[35] To improve accuracy in calculations of the quantum yields, the blue sides of the emission spectra were constructed using the log-normal function as described previously.[34]

Time-Resolved Fluorescence Measurement. Time-resolved intensity decay data were obtained using a HORIBA JobinYvon MF^2 phase/modulation multifrequency domain fluorometer. The excitation wavelength was 295 nm (LED). Emission was detected through a combination of the filters (Semrock LP02-325RS-25 and Corning 7-51) that provide a bandpass of 325−410 nm. *p*-Terphenyl in ethanol was used as a reference standard (τ = 1.05 ns). Data analyses were performed with a nonlinear least-squares program from the Center for Fluorescence Spectroscopy (M. L. Johnson), University of Maryland at Baltimore, School of Medicine (Baltimore, MD). The goodness of fit was assessed by the χ^2 criterion.

The intensity decay data were analyzed in terms of the multiexponential decay law

$$I(t) = \sum_i \alpha_i \exp(-t/\tau_i)$$

where α_i and τ_i are the normalized pre-exponential factors and decay times, respectively. The fractional fluorescence intensity of each component is defined as $f_i = \alpha_i\tau_i/\sum\alpha_j\tau_j$.

Intensity- (mean lifetime) and amplitude-averaged (corresponding to quantum yield) lifetimes were calculated as $\tau_{av} = \sum_i f_i\tau_i$ and $\langle\tau\rangle = \sum_i\alpha_i\tau_i$, respectively.

To reveal the origin of the differences between Trp fluorescence lifetimes, ratios of two lifetimes were arranged to dynamic quenching of the fluorescence and reshuffling between the rotamer populations, as the following formula[36]

$$\frac{\langle\tau\rangle}{\langle\tau_0\rangle} = \frac{\sum\alpha_i\tau_{0i}}{\sum\alpha_{0i}\tau_{0i}} \times \frac{\sum\alpha_i\tau_i}{\sum\alpha_i\tau_{0i}} = f_{PR} \times f_{DQ} \quad (1)$$

where the subscript 0 refers to the reference state and f_{PR} and f_{DQ} represent population reshuffling and pure dynamic quenching, respectively.

RESULTS AND DISCUSSION

All single Trp mutants used in this study were previously characterized and used in solution structure determination of TL by the SDTF method.[5] Newly prepared single Trp mutants of TL have the native fold as evidenced from far-UV CD spectra, which are very similar to those found previously.[5] The agreement of fluorescence λ_{max} values obtained for the mutants in this study with that previously published strongly supports retention of the native fold.

Steady-State Fluorescence Spectroscopy. Steady-state fluorescence measurements on single Trp mutants were performed to evaluate possible correlation between the fluorescence parameters and position of the residue in the α-helix of TL. The log-normal distribution of the corrected fluorescence spectrum of W124, as an example, is shown in Figure 1. The fit was nearly perfect for this and other mutants (not shown). The constructed fluorescence spectra are critical for accurate determination of the quantum yield values (Table 1). Ribbon diagram of TL and fluorescence λ_{max} values of Trp residues located in the α-helix part are shown in Figure 2. The data are consistent with previous findings.[5] The pattern of the fluorescence λ_{max} values along the sequence reveals the periodicity of 3.6 that indicates an α-helix conformation (Figure 2B, dotted line). Fluorescence λ_{max} values perfectly match with positions of the amino acid residues in the protein.

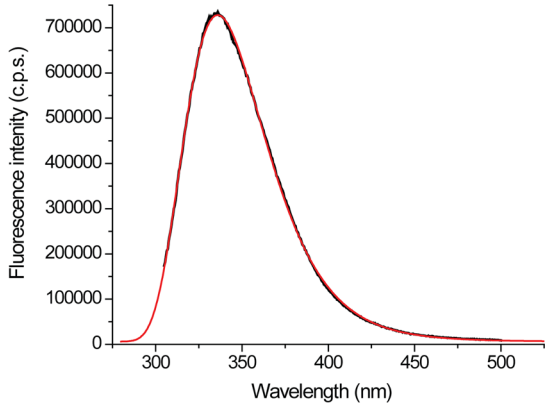

Figure 1. Construction of the corrected fluorescence spectrum for a single Trp mutant. A corrected fluorescence spectrum of W124 (black line) and fitted to log-normal function (red, see Experimental Section) with the extrapolated blue edge.

Indeed, the solvent-exposed positions in the α-helix (positions 125, 128, 132, and 135) correspond to the most red-shifted fluorescence (Figure 2). Fluorescence λ_{max} values of Trp residues in these positions are similar with the average value of 353.1 ± 1.3 nm. The result is expected for solvent-exposed Trp residues located in similar environments.[4] Trp residues located in the opposite side of the α-helix (126, 130, 133, and 137) have tertiary interaction with corresponding residues located in the β-strand H and, therefore, are buried from solvent (Figure 2). These residues display the most blue-shifted fluorescence. However, Trp fluorescence λ_{max} values for the buried residues are more dissimilar with the average value of 333.3 ± 12.1 nm. The high standard deviations for the average values are indicative of both more dispersive fluorescence λ_{max} values and dissimilar environments for the buried residues (tertiary contact).

Time-Resolved Fluorescence and Lifetime Distribution. Because of restriction imposed by the backbone of α-helixes, Trp residues at positions 124−137 (Figure 2) avail the opportunity to test the rotamer model for the fluorescence lifetime distribution. Frequency domain intensity decay curves for the mutants W125 and W130, as representatives of single Trp mutants located in the α-helix, are shown in Figure 3. Fluorescence parameters calculated from the intensity decay analysis of the mutants are shown in Table 1. Among single Trp mutants, fluorescence quantum yield values vary about 4 times. However, κ_r values for these mutants differ by a factor of 1.8 times and most approach that of NATA (calculated from Q = 0.13 and τ = 2.8 ns), 46 × 10^6 s^{-1}. The average radiative rate constant (κ_r) values calculated from all considered Trp residues are (36.7 ± 5.1) × 10^6 s^{-1} and within 20% of the value calculated for NATA. It follows that dynamic quenching is responsible for different quantum yield values. The shortest κ_r value (25.7 × 10^6 s^{-1}), indicative of some quasistatic quenching, observed for Trp at position 133 most likely results from hydrogen bonding between Trp133 and Asp129 (the distance between −NH atom of Trp and OD2 of Asp is 2.1 Å, Figure 4). The fluorescence λ_{max} value of Trp133 points toward a mechanism of quenching. Indeed, one would expect more blue-shifted fluorescence for Trp133, which is located in the middle of the buried side of the α-helix (Figure 2). However, it is known that the negative charge near the pyrrole end (where NH− group resides) of the indole ring creates a red shift of the fluorescence.[7] Therefore, the relatively red-shifted fluorescence (λ_{max}= 340 nm) and the short κ_r value observed for Trp133 support its putative position with respect to Asp129 (Figure 4). Similarly, other buried Trp residues show decreased fluorescence quantum yields and lifetimes. Average lifetimes of the buried Trp residues (tertiary interaction side) display about a 31% decreased value compared to that of the exposed side. This is true particularly for shorter lifetime components. The average quantum yields of Trp residues located in the solvent exposed and buried sides of α helix (Figure 2) are 0.15 ± 0.06 and 0.06 ± 0.01, respectively. Solving the ratio of average $\langle\tau\rangle$ values for solvent exposed and buried sides using the formula 1 returns 0.66 and 0.80 values for f_{PR} and f_{DQ}, respectively. The result indicates that both population reshuffling and dynamic quenching play a role in diminished average lifetime or quantum yield in the buried side of the α helix. Population reshuffling predominates.

A large body of evidence indicates that multiexponential fluorescence decays of single Trp residues in proteins and conformationally restricted peptides, generally, result from

dx.doi.org/10.1021/jp309318r | J. Phys. Chem. B 2012, 116, 13381−13388

Table 1. Fluorescence Lifetime Parameters for Single Trp Mutant Located in the α-Helix of Human Tear Lipocalin at pH 7.3

mutant	[a]α_1	α_2	α_3	[b]τ_1 (ns)	τ_2 (ns)	τ_3 (ns)	[c]τ_{av} (ns)	[d]$\langle\tau\rangle$ (ns)	[e]Q	[f]$\kappa_r \times 10^{-6}(s^{-1})$	χ^2
Trp124	0.59 (0.02)	0.41 (0.02)		1.12 (0.03)	3.01 (0.07)		2.35 (0.14)	1.89 (0.07)	0.07	38.6	0.5
[g]Trp124	0.42 (0.03)	0.56 (0.02)	0.02 (0.00)	0.85 (0.06)	2.44 (0.08)	8.25 (0.71)	2.65 (0.55)	1.89 (0.14)	0.07	38.6	0.3
Trp125	0.18 (0.01)	0.82 (0.01)		1.49 (0.07)	6.07 (0.02)		5.84 (0.10)	5.25 (0.07)	0.21	40.4	0.4
Trp126	0.70 (0.01)	0.30 (0.01)		0.94 (0.03)	4.19 (0.08)		3.07 (0.14)	1.92 (0.05)	0.06	31.5	0.9
[g]Trp126	0.56 (0.01)	0.36 (0.01)	0.08 (0.02)	0.66 (0.05)	2.53 (0.20)	6.83 (0.43)	3.44 (0.97)	1.83 (0.26)	0.06	33.0	0.5
Trp127	0.38 (0.02)	0.62 (0.02)		1.79 (0.07)	4.58 (0.05)		4.04 (0.18)	3.52 (0.11)	0.16	46.3	0.5
Trp128	0.25 (0.01)	0.75 (0.02)		1.73 (0.08)	5.71 (0.03)		5.34 (0.19	4.72 (0.12)	0.17	36.0	0.5
Trp129	0.22 (0.01)	0.78 (0.01)		1.29 (0.08)	6.28 (0.05)		6.01 (0.13)	5.18 (0.08)	0.21	40.6	0.6
Trp130	0.84 (0.01)	0.16 (0.01)		1.14 (0.02)	3.84 (0.09)		2.20 (0.12)	1.57 (0.05)	0.05	33.6	0.5
Trp131	0.39 (0.00)	0.61 (0.00)		1.07 (0.03)	4.27 (0.02)		3.83 (0.03)	3.02 (0.02)	0.11	37.7	0.4
Trp132	0.53 (0.01)	0.47 (0.01)		0.90 (0.02)	3.25 (0.03)		2.69 (0.08)	2.00 (0.04)	0.07	33.8	0.5
Trp133	0.59 (0.01)	0.41 (0.00)		0.79 (0.02)	5.22 (0.04)		4.43 (0.06)	2.61 (0.02)	0.07	25.7	0.6
Trp134	0.44 (0.01)	0.43 (0.01)	0.13 (0.01)	0.39 (0.05)	1.78 (0.10)	4.64 (0.14)	2.75 (0.24)	1.54 (0.08)	0.07	42.5	0.4
Trp135	0.32 (0.00)	0.68 (0.00)		0.93 (0.03)	5.29 (0.02)		4.96 (0.03)	3.89 (0.02)	0.14	36.8	0.4
Trp136	0.34 (0.01)	0.66 (0.01)		1.50 (0.04)	4.91 (0.04)		4.45 (0.06)	3.75 (0.03)	0.15	41.1	0.3
Trp137	0.61 (0.01)	0.39 (0.01)		0.97 (0.02)	3.23 (0.05)		2.51 (0.09)	1.85 (0.04)	0.06	34.7	0.6
[h]Trp^{all}	*0.45 (0.19)*	*0.55 (0.19)*		*1.18 (0.34)*	*4.56 (1.17)*		*4.00 (1.30)*	*3.17 (1.32)*	*0.12 (0.06)*	*36.7 (5.1)*	
Trp^{exp}	*0.32 (0.15)*	*0.68 (0.15)*		*1.26 (0.41)*	*5.08 (1.26)*		*4.71 (1.39)*	*3.97 (1.42)*	*0.15 (0.06)*	*36.8 (2.7)*	
Trp^{bur}	*0.65 (0.13)*	*0.33 (0.12)*		*0.96 (0.14)*	*4.12 (0.83)*		*3.05 (0.99)*	*1.99 (0.44)*	*0.06 (0.01)*	*31.4 (4.0)*	

[a]Normalized pre-exponential factor. [b]Decay time. [c]Intensity-averaged lifetime. [d]Amplitude-averaged lifetime. [e]Quantum yield. [f]Radiative rate constant, Trp^{all} represents average value from all sites. [g]In triple-exponential models, these sites reveal minimal contributions for the third (long lifetime) components and insignificant improvement of the goodness of fit. Trp^{exp} represent average value from exposed sites (positions 125, 128, 132, and 135); Trp^{bur} represent the average value from buried (tertiary interaction) sites (126, 130, 133, and 137). [h]Because of three lifetime components, W134 was excluded from calculation. Italicized numbers indicate average values. The numbers in parentheses are the standard deviations.

dx.doi.org/10.1021/jp309318r | J. Phys. Chem. B 2012, 116, 13381−13388

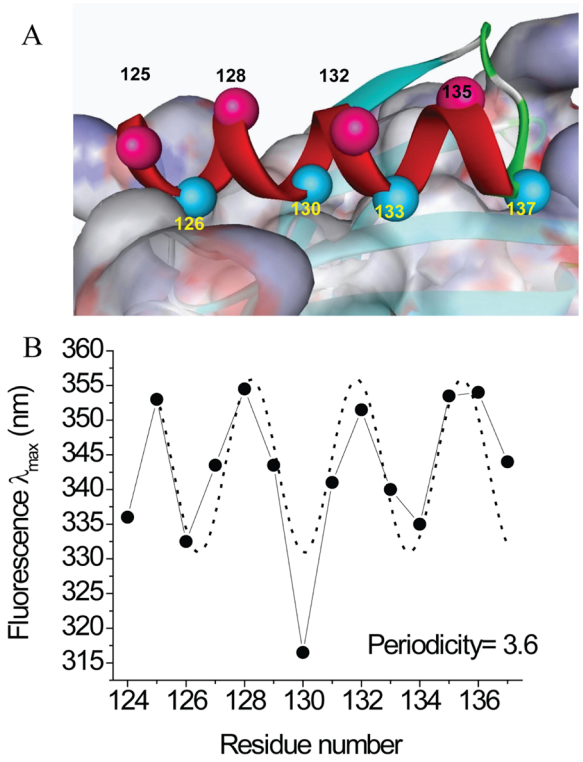

Figure 2. Correspondence of fluorescence λ_{max} values and the locations of Trp residues in TL. (A) Ribbon diagram of the α-helix segment of TL selected for the fluorescence study. Red-magenta and blue balls represent the location of the C_α-atoms in the solvent exposed and buried (tertiary interaction) sides of the α-helix, respectively. (B) Fluorescence λ_{max} values of single Trp residues located in the α-helix segment of TL. The dotted line represents the fitting curve for the α-helical content with periodicity of 3.6.The ribbon diagram of TL was generated from the PDB file (3EYC) with DS Visualizer 2.5 (Accelrys Inc.).

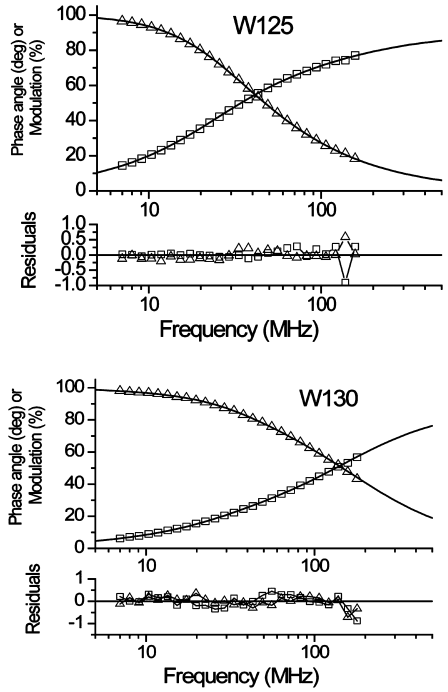

Figure 3. Phase angle (squares) and modulation (triangles) fluorescence lifetime data of TL mutant W125 and W130 at pH 7.3. Solid lines represent the best biexponential fit for the parameters given in Table 1.

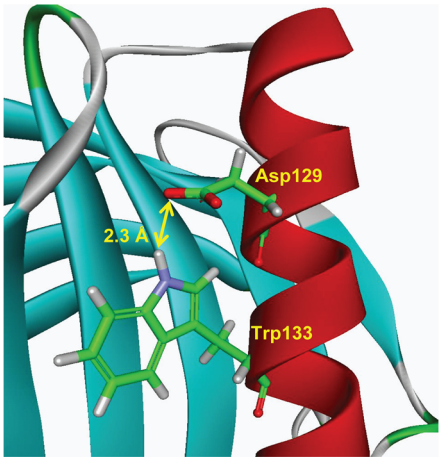

Figure 4. Relative orientations of Trp133 and Asp129 in the α-helical segment of TL. The mutation to introduce Trp at position 133 and rotamer assignment were generated from the PDB file (3EYC) with DS Visualizer 2.5 (Accelrys Inc.).

ground-state heterogeneity, i.e., rotamers. Commonly, triple-exponential decays observed in single-tryptophan proteins have been linked to χ_1 (+60 (g^+); 180 (t); −60 (g^-)) rotamers. It is widely accepted that the rotamer model can be safely employed if conformer interconversion is much slower than the fluorescence lifetime scale. Generally, this is the case when Trp is positioned in a rigid backbone, such as the α-helix considered in this study. In the regular α-helix steric conflict with the $i - 3$ backbone atom precludes the χ_1 = +60 rotamer for tryptophan residues. Therefore, Trp in the α-helix should be limited to two fluorescence lifetimes if the rotamer model is valid. Indeed, the fluorescence lifetime parameters of Trp residues in the α-helix of TL (Figure 2) reveal mostly two lifetime components (Table 1). Only Trp134 indicates a significant contribution for a third component that improves the goodness of fit.

In situations where conformer interconversion is much faster, the rotamer model is not applicable and fluorescence decay collapses to a single exponential.[10] This is not the case for single Trp mutants located in the α-helix (Table 1). The situation is more complicated when conformer interconversion occurs on the fluorescence time scale. Such cases were analyzed as an excited-state reaction scheme by different groups.[10,37] It was pointed out that a very short decay time with a small amplitude is a sign of conformer interconversion within the time frame of fluorescence decay.[10] Pre-exponential values for shorter lifetimes in the solvent exposed side (average is 0.32 ± 0.15) are smaller than those observed for the buried side (average is 0.65 ± 0.13). However, the average lifetime for the short lifetime components (1.26 ± 0.41 ns) in the solvent exposed side is somewhat greater compared to that of the buried side (0.96 ± 0.14 ns) (Table 1). Therefore, the rotamer interconversion process can be safely excluded for Trp residues located in the α-helix. The results obtained for single Trp residues located in the amphipathic peptides corroborate this conclusion.[18] Conformer interconversions were not detected even in the unstructured conformations of the peptides. The authors noted that average pre-exponential factors of the three lifetimes, which also include short-lifetime components, agreed

dx.doi.org/10.1021/jp309318r | J. Phys. Chem. B 2012, 116, 13381−13388

well with average χ_1 distributions of Trp residues located in unstructured structures derived from X-ray crystallographic data of the proteins.[18] The results obtained for the peptides in α-helix conformation were even more convincing. Only two lifetimes were observed for all Trp residues located in the α-helix conformation of the peptides.[18] More importantly, average pre-exponential factors (0.7) for relatively short lifetimes (average value is about 2.7 ns) were much higher compared to that observed for the long lifetimes, 0.3 for average lifetimes of 7.0 ns. If interconversion exists, the opposite tendency should be observed. For the peptide in an α-helical conformation, the same rotamer distribution as indicated above was observed regardless of whether Trp residues were located in the solvent exposed sites or in bound sites to the phospholipid bilayer. On the basis of the correspondence between the pre-exponential factors of Trp fluorescence decays and Trp rotamer distributions in the α-helix in proteins, the authors concluded that short (2.7 ns) and long (7.0 ns) lifetimes correspond to t and g^- rotamers. Our data support this assignment. However, there are important differences.

Both fluorescence and structural properties of Trp 130 allow the rotamer assignment of the fluorescence lifetimes. Trp 130 shows most blue-shifted fluorescence in TL with λ_{max} of 316.5 nm. Previously, based on the steady-state fluorescence and CD data, it was stated that the side chain of the Trp at position 130 is sandwiched between two hydrophobic residues of the β-strand H, Val113 and Leu115 (Figure 5).[5] This is possible only

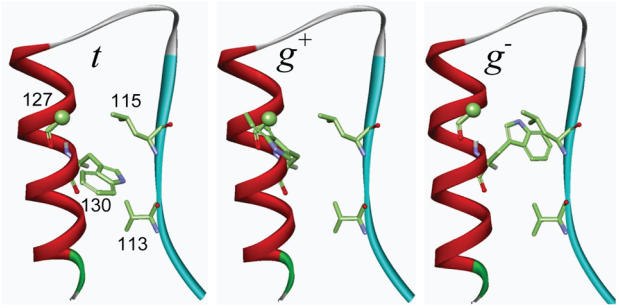

Figure 5. χ_1 rotamers of Trp130 in the α-helix of TL. The rotamer t is in the original conformation (native Phe 130) that is sandwiched between the residues Val 113 and Ile 115; the rotamer g^- has a clash with the backbone of the residue $i - 3$ (Leu127); the rotamer g^+ has a clash with the side chain of Val 115. Green balls depict the position of the C^α-atom.

in the t-rotamer conformation. This conformation was later confirmed for the original residue Phe 130 by crystallographic studies of TL.[20,21] As mentioned above, the g^+ rotamer is improbable because of steric conflict with backbone atom of the residue $i - 3$, i.e., Leu127 (Figure 5). The rotamer g^- creates conflict with the side chain of the residue Leu115. In this conformation, there should be some alteration in packing elements in order circumvent the steric conflict with Leu115. Therefore, the side chain of Trp at position 130 should predominantly have the t rotamer. Indeed, fluorescence intensity decay analysis of Trp130 indicates that the lifetime component of 1.14 ns has a pre-exponential factor 0.84 (Table 1), which supports the assignment as a t rotamer. Time-resolved fluorescence and NMR data obtained on the cyclic hexapeptides[11] also buttress this assignment. The peptides showed three fluorescence lifetimes about 3.8, 1.8, and 0.3 ns, of which 3.8 and 1.8 ns were assigned to the g^- and t rotamers, respectively. The lifetime component of 3.84 ns with pre-exponential value of 0.16 could only be assigned to g^- rotamer if some alteration in the structure of TL is stipulated. Thus, 84% of Trp 130 assumes the t rotamer conformation. This assignment supports the interpretation of fluorescence lifetime distribution in the α-helical peptide. However, in TL unlike the peptide, Trp side-chain rotamer populations differ for various sites.

In the solvent-exposed side of the α-helix (residues 125, 128, 132, and 135) the average pre-exponential factors for short- and long-lifetime components are 0.32 ± 0.15 and 0.68 ± 0.15, respectively. The average lifetimes for these components are 1.41 ± 0.35 and 4.99 ± 1.25 ns (Table 1). However, in the buried side of the α-helix (residues 126, 130, 133, and 137) the average pre-exponential factors for the short- and long-lifetime components are 0.65 ± 0.13 and 0.33 ± 0.12, respectively. The opposite situation is observed for the solvent-exposed side. The average lifetimes of Trp fluorescence for the buried side are 0.96 ± 0.14 and 4.12 ± 0.83 ns. Thus, only Trp residues located in the buried side of the α-helix of TL show very similar rotamer distributions to that observed in the model peptide with α-helical conformation. Comparison of the rotamer distribution assigned from Trp fluorescence to that found by X-ray crystallography is informative. One of the rotamer libraries (total of 140 α-helical Trp side-chain rotamers in the data set) reveals the following distribution: g^+ = 3%, t = 56%, and g^- = 37%.[38] In the current study, which was performed in solution, the t rotamer is dominant only in buried residues (tertiary interaction side) (Table 1). The fluorescence intensity decay parameters for the buried side indicate that on average about 65% of the side chains of Trp residues populate the t rotamer. It is reasonable, because in the t rotamer conformation the side chain of Trp can efficiently interact with the residues located in the opposing β-strand (Figure 5). A recently described very comprehensive rotamer library facilitates the understanding of the rotamer distribution data for the exposed side of the α-helix obtained from the fluorescence study.[39] The fluorescence decay parameters (Table 1) indicate that in the solvent exposed side, the g^- rotamer is dominant (about 68% population). Figure 6 shows data recovered from the rotamer library.[39] As can be seen, Trp rotamer distribution depends on backbone conformation even within α-helix structure (Figure 6). Although overall dominance of the t rotamer is obvious, in conformations where Psi is <35° the rotamer g^- becomes more probable (Figure 6). Therefore, for some regions of the α-helix, rotamer g^- could be dominant. It should be noted that dependence of the rotamer distribution on the ϕ angles is not so obvious (Figure 6). Currently, we do not have enough data for statistical analysis to analyze dependence of pre-exponential values of Trp fluorescence on ϕ angles in the α-helix. However, as mentioned previously[40] rotamer libraries use crystal structures instead of solution structures and may suffer from artifacts induced by crystal packing. It is also possible that replacing amino acids to Trp may only slightly modify ϕ and ψ angles keeping their intact α-helix conformation.

RD-SDTF (rotamer distribution for site directed tryptophan fluorescence) extends the power of the standard SDTF technique. Currently, both site-directed spin labeling and SDTF rely on site-specific differences (accessibility to solvent, mobility, polarity, etc.) for solution structure determination.[5,41,42] These features will be readily determined if one side of the α-helix interacts with another part of the protein, Figure 5. However, if all sites of the α-helix are exposed to the

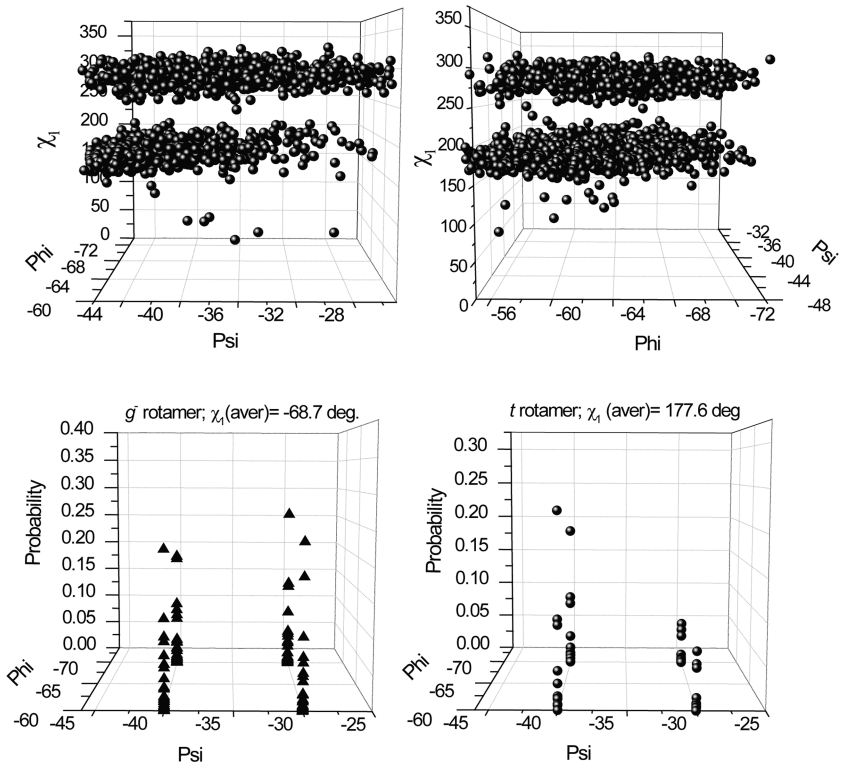

Figure 6. Distribution of Trp side-chain rotamers in the α-helix of proteins. Populations (A and B, upper) and probability (C and D, lower) of distribution of Trp side chains in backbone conformation in the range relevant to the α-helix of TL. The 5% smoothed rotamer library provided by R.L. Dunbrack's group (http://dunbrack.fccc.edu/bbdep2010) was used to generate the figures. For clarity, the g^+ rotamers, which are only possible in the N-terminal end of the α-helix, were removed from (A) and (B). Data around χ_1 = 300° represent g^- rotamers.

solvent then these methodologies are rendered useless. Ability to discriminate Trp rotamers from fluorescence intensity decay experiments removes that limitation for SDTF.

RD-SDTF could be applied to membrane proteins, which are rich with α-helix motif. They are a very important class of proteins, which are responsible for transporting ions and molecules across the membrane, participating in signal transduction, and light harvesting.[43] Membrane proteins represent less than 2% of the Protein Data Bank because of difficulties to obtain high-resolution structures.[44] Therefore, a method that could resolve structure and dynamics of the proteins, as well as membrane proteins, particularly in solution is very important. As mentioned above, the RD-SDTF technique does not rely on environmental differences of side chains in α-helix. It uses rotamer assignment of the Trp fluorescence lifetimes in which g+ rotamer is not feasible for α-helical segments. This method could also be helpful to validate structure assignment used in regular SDTF and, potentially, pinpoint α-helix bending, observed in many α-helical transmembrane proteins.

AUTHOR INFORMATION

Corresponding Author

*Phone: (310) 825-6261 (O.K.G.); (310) 825-6998 (B.J.G.). Fax: (310) 794-2144 (O.K.G.); (310) 794-2144 (B.J.G.). E-mail: ogassymov@mednet.ucla.edu (O.K.G.); bglasgow@mednet.ucla.edu (B.J.G.).

Notes

The authors declare no competing financial interest

ACKNOWLEDGMENTS

This work was supported by U.S. Public Health Service grants NIH EY11224 and EY00331 as well as the Edith and Lew Wasserman Endowed Professorship in Ophthalmology (B.G.).

ABBREVIATIONS

CD, circular dichroism; ET, electron transfer; NGAL, neutrophil gelatinase-associated lipocalin; NATA, *N*-acetyl-L-tryptophanamide; RD-SDTF, rotamer distribution with SDTF; SDTF, site-directed tryptophan fluorescence; TL, human tear lipocalin

REFERENCES

(1) Goetz, D. H.; Holmes, M. A.; Borregaard, N.; Bluhm, M. E.; Raymond, K. N.; Strong, R. K. *Mol. Cell* **2002**, *10*, 1033−1043.
(2) Correnti, C.; Clifton, M. C.; Abergel, R. J.; Allred, B.; Hoette, T. M.; Ruiz, M.; Cancedda, R.; Raymond, K. N.; Descalzi, F.; Strong, R. K. *Structure* **2011**, *19*, 1796−1806.
(3) Gasymov, O. K.; Abduragimov, A. R.; Glasgow, B. J. *Biochemistry* **2012**, *51*, 2991−3002.
(4) Lakowicz, J. R. *Principles of Fluorescence Spectroscopy*, 3rd ed.; Springer: New York, 2006.
(5) Gasymov, O. K.; Abduragimov, A. R.; Yusifov, T. N.; Glasgow, B. J. *Biochemistry* **2001**, *40*, 14754−14762.
(6) Pan, C. P.; Callis, P. R.; Barkley, M. D. *J. Phys. Chem. B* **2006**, *110*, 7009−7016.
(7) Vivian, J. T.; Callis, P. R. *Biophys. J.* **2001**, *80*, 2093−2109.
(8) Chen, Y.; Barkley, M. D. *Biochemistry* **1998**, *37*, 9976−9982.
(9) Chen, Y.; Liu, B.; Yu, H. T.; Barkley, M. D. *J. Am. Chem. Soc.* **1996**, *118*, 9271−9278.
(10) McMahon, L. P.; Yu, H.-T.; Vela, M. A.; Morales, G. A.; Shui, L.; Fronczek, F. R.; McLaughlin, M. L.; Barkley, M. D. *J. Phys. Chem. B* **1997**, *101*, 3269−3280.

(11) Adams, P. D.; Chen, Y.; Ma, K.; Zagorski, M. G.; Sonnichsen, F. D.; McLaughlin, M. L.; Barkley, M. D. *J. Am. Chem. Soc.* **2002**, *124*, 9278−9286.
(12) Pan, C. P.; Muino, P. L.; Barkley, M. D.; Callis, P. R. *J. Phys. Chem. B* **2011**, *115*, 3245−3253.
(13) Callis, P. R.; Petrenko, A.; Muino, P. L.; Tusell, R. *J. Phys. Chem. B* **2007**, *111*, 10335−10339.
(14) Vivian, J. T.; Callis, P. R. *Biophys. J.* **2001**, *80*, 2093−2109.
(15) Pan, C. P.; Barkley, M. D. *Biophys. J.* **2004**, *86*, 3828−3835.
(16) Liu, B.; Thalji, R. K.; Adams, P. D.; Fronczek, F. R.; McLaughlin, M. L.; Barkley, M. D. *J. Am. Chem. Soc.* **2002**, *124*, 13329−13338.
(17) Callis, P. R.; Liu, T. *J. Phys. Chem. B* **2004**, *108*, 4248−4259.
(18) Clayton, A. H. A.; Sawyer, W. H. *Biophys. J.* **1999**, *76*, 3235−3242.
(19) Gasymov, O. K.; Abduragimov, A. R.; Glasgow, B. J. *Biochemistry* **2010**, *49*, 582−590.
(20) Breustedt, D. A.; Chatwell, L.; Skerra, A. *Acta Crystallogr. D: Biol. Crystallogr.* **2009**, *65*, 1118−1125.
(21) Breustedt, D. A.; Korndorfer, I. P.; Redl, B.; Skerra, A. *J. Biol. Chem.* **2005**, *280*, 484−493.
(22) Flower, D. R. *Biochem. J.* **1996**, *318* (Pt1), 1−14.
(23) Glasgow, B. J.; Abduragimov, A. R.; Farahbakhsh, Z. T.; Faull, K. F.; Hubbell, W. L. *Curr. Eye Res.* **1995**, *14*, 363−372.
(24) Dean, A. W.; Glasgow, B. J. *Invest. Ophthalmol. Vis. Sci.* **2012**, *53*, 1773−1782.
(25) Gasymov, O. K.; Abduragimov, A. R.; Yusifov, T. N.; Glasgow, B. J. *Biochim. Biophys. Acta* **1999**, *1433*, 307−320.
(26) Glasgow, B. J.; Gasymov, O. K.; Abduragimov, A. R.; Yusifov, T. N.; Altenbach, C.; Hubbell, W. L. *Biochemistry* **1999**, *38*, 13707−13716.
(27) Glasgow, B. J.; Gasymov, O. K.; Abduragimov, A. R.; Engle, J. J.; Casey, R. C. *Invest. Ophthalmol. Vis. Sci.* **2010**, *51*, 1981−1987.
(28) Gasymov, O. K.; Abduragimov, A. R.; Yusifov, T. N.; Glasgow, B. J. *Biochim. Biophys. Acta* **1998**, *1386*, 145−156.
(29) Gasymov, O. K.; Abduragimov, A. R.; Yusifov, T. N.; Glasgow, B. J. *Biochemistry* **2002**, *41*, 8837−8848.
(30) Glasgow, B. J.; Heinzmann, C.; Kojis, T.; Sparkes, R. S.; Mohandas, T.; Bateman, J. B. *Curr. Eye Res.* **1993**, *12*, 1019−1023.
(31) Redl, B.; Holzfeind, P.; Lottspeich, F. *J. Biol. Chem.* **1992**, *267*, 20282−20287.
(32) Glasgow, B. J. *Graefes Arch. Clin. Exp. Ophthalmol.* **1995**, *233*, 513−522.
(33) Cormack, B. In *Current Protocol in Molecular Biology*; Greene Pub. Associates and Wiley-Interscience: New York, 1987; Suppl. 15.
(34) Gasymov, O. K.; Abduragimov, A. R.; Yusifov, T. N.; Glasgow, B. J. *Biochemistry* **2004**, *43*, 12894−12904.
(35) Lehrer, S. S. *Biochemistry* **1971**, *10*, 3254−3263.
(36) Kuppens, S.; Hellings, M.; Jordens, J.; Verheyden, S.; Engelborghs, Y. *Protein Sci.* **2003**, *12*, 930−938.
(37) Donzel, B.; Gauduchon, P.; Wahl, P. *J. Am. Chem. Soc.* **1974**, *96*, 801−808.
(38) Lovell, S. C.; Word, J. M.; Richardson, J. S.; Richardson, D. C. *Proteins* **2000**, *40*, 389−408.
(39) Shapovalov, M. V.; Dunbrack, R. L. *Structure* **2011**, *19*, 844−858.
(40) Scouras, A. D.; Daggett, V. *Protein Sci.* **2011**, *20*, 341−352.
(41) McHaourab, H. S.; Lietzow, M. A.; Hideg, K.; Hubbell, W. L. *Biochemistry* **1996**, *35*, 7692−7704.
(42) Gasymov, O. K.; Abduragimov, A. R.; Yusifov, T. N.; Glasgow, B. J. *Biochem. Biophys. Res. Commun.* **1997**, *239*, 191−196.
(43) Marsico, A.; Henschel, A.; Winter, C.; Tuukkanen, A.; Vassilev, B.; Scheubert, K.; Schroeder, M. *BMC Bioinf.* **2010**, *11*, 204.
(44) Bowie, J. U. *Nature* **2005**, *438*, 581−589.